

## Article

# Palladium-Catalyzed Decarbonylative Nucleophilic Halogenation of Acid Anhydrides

Tian Tian <sup>1</sup>, Shuhei Uei <sup>2</sup>, Weidan Yan <sup>1</sup> and Yasushi Nishihara <sup>3,\*</sup> 
<sup>1</sup> Graduate School of Natural Science and Technology, Okayama University, 3-1-1 Tsushimanaka, Kita-ku, Okayama 700-8530, Japan; tian\_tian@s.okayama-u.ac.jp (T.T.); poo1662y@s.okayama-u.ac.jp (W.Y.)

<sup>2</sup> Department of Chemistry, Faculty of Science, Okayama University, 3-1-1 Tsushimanaka, Kita-ku, Okayama 700-8530, Japan; puu18kuj@s.okayama-u.ac.jp

<sup>3</sup> Research Institute for Interdisciplinary Science (RIIS), Okayama University, 3-1-1 Tsushimanaka, Kita-ku, Okayama 700-8530, Japan

\* Correspondence: ynishiha@okayama-u.ac.jp; Tel.: +81-86-251-7855

**Abstract:** In this study, we developed a palladium-catalyzed decarbonylative nucleophilic halogenation reaction using inexpensive and readily available acid anhydrides as substrates. This approach effectively circumvents the instability of acyl chlorides and the low reactivity of acyl fluorides. The Pd/Xantphos catalyst system exhibited excellent compatibility with the thermodynamically and kinetically challenging reductive elimination of C–X bonds (X = I, Br, and Cl) from Pd(II) intermediates. Notably, for electron-donating substrates, adopting an open system significantly improved the reaction efficiency. The positive effect of the open system may be due to the reversible nature of CO insertion and deinsertion, which helps direct the reaction toward the desired pathway by allowing the generated CO to exit the reaction system. Mechanistic studies suggest that the reaction proceeds through a highly reactive acyl halide intermediate, followed by a unimolecular fragment coupling (UFC) pathway via decarbonylation or an alternative pathway involving the formation of an activated anionic palladate complex in the presence of lithium halide.

**Keywords:** reductive elimination of C–X bond; nucleophilic halogenation; unimolecular fragment coupling (UFC); acid anhydrides; aryl halides



Academic Editors: Erqing Li and Yue Wang

Received: 5 February 2025

Revised: 12 February 2025

Accepted: 17 February 2025

Published: 19 February 2025

**Citation:** Tian, T.; Uei, S.; Yan, W.; Nishihara, Y. Palladium-Catalyzed Decarbonylative Nucleophilic Halogenation of Acid Anhydrides. *Catalysts* **2025**, *15*, 191. <https://doi.org/10.3390/catal15020191>

**Copyright:** © 2025 by the authors. Licensee MDPI, Basel, Switzerland. This article is an open access article distributed under the terms and conditions of the Creative Commons Attribution (CC BY) license (<https://creativecommons.org/licenses/by/4.0/>).

## 1. Introduction

Aryl halides are highly versatile building blocks in organic synthesis and play a crucial role in various chemical research fields, including pharmaceuticals [1,2], organic functional materials [3], natural product total synthesis [4,5], agricultural and pesticide development [6], and molecular recognition [7], due to the highly polarized C–X bonds and good leaving properties of halogen atoms. Notably, aryl halides readily undergo oxidative addition under transition metal catalysis to form Ar–[TM]–X complexes [8–10], where TM: transition metals, X: halogen atoms, participate in one-electron transfer in reducing systems to generate aryl radicals and organometallic species [11–13] and serve as precursors for high-valent halogenating agents upon oxidation [14–17]. In particular, highly reactive aryl iodides and bromides are frequently used as electrophiles and serve as key coupling partners in cross-coupling reactions. However, their synthesis presents challenges, including functional-group compatibility, and commercially available aryl halides remain limited. Among them, aryl iodides account for only 2% of all commercially available aryl halides and are relatively expensive [18]. Therefore, developing efficient and cost-effective methods for synthesizing aryl halides—especially aryl iodides and

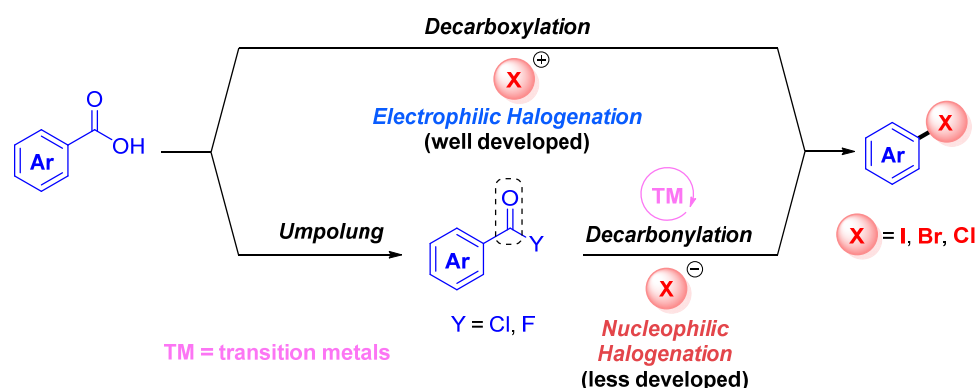
bromides—from inexpensive and widely available starting materials is an urgent and important research goal.

On the other hand, carboxylic acids and their derivatives—many of which are inexpensive and readily available—have recently attracted significant research interest for their potential in synthetic transformations [19,20]. In particular, the well-known Hunsdiecker–Borodin decarboxylative electrophilic halogenation of carboxylic acids has been extensively developed over the past two decades as an efficient approach for synthesizing aromatic halides [21–23]. This method employs highly reactive electrophilic halogenating agents, often in combination with nucleophilic halogen sources and oxidants, to facilitate the decarboxylation process while introducing a halogen atom instead of the carboxyl group [24]. Due to the unique reactivity of this transformation, carboxylic acids can be considered as activating groups for the synthesis of organic halides, offering a straightforward and cost-effective strategy that aligns with the principles of modern organic synthesis (Figure 1a, top). Although decarboxylative halogenation using carboxylic acids as substrates is an ideal transformation, it remains challenging to overcome numerous limitations. In particular, unlike aliphatic carboxylic acids, aromatic carboxylic acids—which are relatively stable—are known to undergo electrophilic halogenation via decarboxylation with difficulty. Furthermore, many existing decarboxylative halogenation reactions rely on stepwise processes [25] that require toxic metals, highly corrosive or strongly oxidizing reagents [26,27], and complex electrophilic halogenating agents. Additionally, the use of environmentally unfriendly halogenating solvents [28–30], along with cumbersome product purification, further limits the practicality of these methods [24]. While some protocols employing transition metal catalysis have mitigated certain challenges, they have yet to provide a comprehensive solution to these inherent limitations [31,32]. In addition, these reactions often require complex catalytic systems that are not commercially available [33,34], and their poor selectivity leads to the formation of undesirable byproducts [35–38].

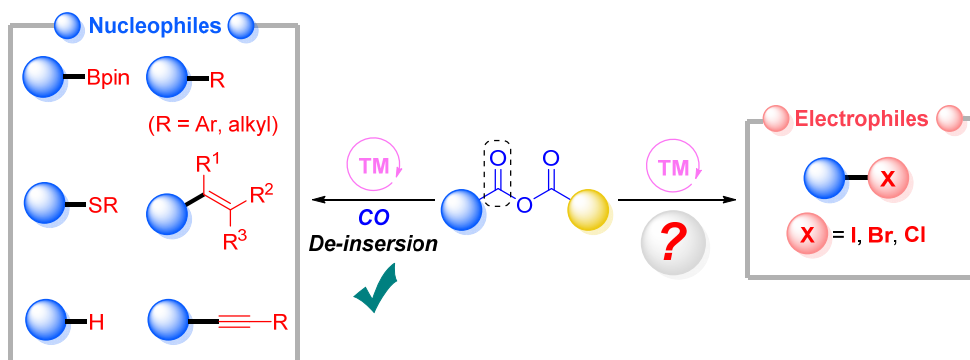
In contrast, the transition-metal-catalyzed nucleophilic decarboxylative halogenation of carboxylic acid derivatives offers a promising solution to these challenges (Figure 1a, bottom). However, two major obstacles must be overcome in designing this reaction. The first issue is that the ligand exchange reaction at the transition metal center will not proceed unless the nucleophilicity of the halogenating agent is sufficiently strong. The second is that the thermodynamically unfavorable reductive elimination of the C–X bond is achieved through the transition metal complex [39–41]. Regarding the second issue, it was previously believed that reductive elimination of the C–X bond via a stoichiometric palladium complex was not feasible. However, in 1987, Echavarren and Stille observed this process [42], and in 2001, Hartwig further demonstrated that it could be achieved using a relatively bulky phosphine ligand [43–45]. Despite the discovery of stoichiometric reactions, their catalytic applications remain minimal due to the relatively low equilibrium constants for C–I bond formation compared to other carbon–halogen bonds. For example, Buchwald and co-workers successfully developed palladium-catalyzed nucleophilic bromination [46], chlorination [47], and even fluorination for aromatic triflates via reductive elimination of the carbon–halogen bond from the transition metal center, using innovative ligand design [48]. They employed *t*-BuBrettPhos, a ligand with unique hemilabile properties that facilitated reductive elimination of the corresponding C–X bonds. However, in contrast, the catalytic formation of C–I bonds has not yet been achieved. To date, Lautens [41,49,50], Tong [51–53], Morandi [54,55], and Xi [56] have made significant progress in promoting C–I bond reductive elimination via carbiodination of unsaturated bonds, successfully synthesizing a range of C(alkyl)–I and C(alkenyl)–I bonds. This success is likely since alkyl and alkenyl iodides are less prone to oxidative addition. However, the catalytic

formation of C(aryl)–I bonds remains a major challenge, requiring further innovation and breakthroughs.

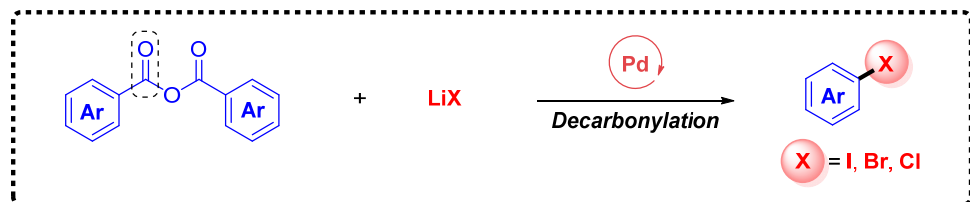
**(a) Decarboxylative/Decarbonylative Halogenation of Carboxylic Acids and Their Derivatives**



**(b) Transition-metal-catalyzed Decarbonylative Transformations of Acid Anhydrides**



**(c) Pd-catalyzed Decarbonylative Nucleophilic Halogenation of Acid Anhydrides (This Work)**



- ★ Practical and cost-effective halide sources
- ★ Inexpensive and readily available carboxylic acid anhydrides
- ★ Broad substrate tolerance for electron-donating groups
- ★ High compatibility with Pd(II)-mediated reductive elimination of C–X bonds

**Figure 1.** (a) Electrophilic and nucleophilic halogenation of carboxylic acids and their derivatives, (b) transition-metal-catalyzed decarbonylative transformations, and (c) decarbonylative nucleophilic halogenation of acid anhydrides (this work).

Transition-metal-catalyzed decarbonylation of carboxylic acid derivatives has been systematically investigated in recent years [57–60]. Nevertheless, due to the chemical instability of acyl chlorides and the low reactivity of esters and amides, chemists have turned to acyl fluorides as novel electrophiles that offer both reactivity and stability. Building on Schoenebeck’s pioneering work on transition-metal-catalyzed decarbonylation [61], our group [62–72] and others [73–83] have recently developed a series of decarbonylative transformations of acyl fluorides, demonstrating their potential for constructing carbon–carbon and carbon–heteroatom bonds. However, the synthesis of acyl

fluorides requires relatively expensive fluorinating agents, which limits their broader application. To address this, acid anhydrides—often referred to as “activated carboxylic acids”—offer a balance of cost-effectiveness, moderate reactivity, and stability in organic synthesis as inexpensive and stable electrophiles. Since Blum and Lipshes first reported the intramolecular decarbonylative cyclization of acid anhydrides using Wilkinson’s catalyst in 1969 [84], transition metal-catalyzed decarbonylation of acid anhydrides has been extensively explored. These transformations have played a crucial role in various reaction pathways, including elimination [85,86], insertion, cyclization [87–89], C–H bond functionalization [90–94], and cross-coupling reactions (Figure 1b). In particular, decarbonylative cross-coupling reactions of acid anhydrides have been successfully identified in reactions such as Mizoroki–Heck coupling [95,96], Negishi coupling [97], Suzuki–Miyaura coupling [98,99], Sonogashira–Hagihara coupling [100–102], Miyaura–Ishiyama borylation [103–105], thioetherification [106,107], and reduction [108]. Importantly, acid anhydrides readily undergo oxidative addition and decarbonylation under transition metal catalysis, enabling a wide range of subsequent transformations [109–113]. As a result, various new nucleophilic reagents have been synthesized. However, the construction of new electrophilic reagents, particularly aryl halides, using the decarbonylation of acid anhydrides, remains an unexplored area of research.

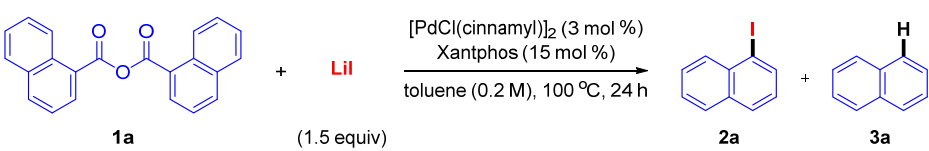
Recently, a significant breakthrough in this research field was achieved by Morandi [114,115] and Arndtsen [116]. They reported a series of well-known metathesis or decarbonylation reactions of organoiodides with acyl chlorides to achieve Pd-catalyzed synthesis of aryl iodides via reductive elimination of the C(Ar)–I bond. On the other hand, we have recently revealed the decarbonylative nucleophilic halogenation of acyl fluorides and chlorides using a Pd/Xantphos catalyst [117]. This reaction system employs alkali metal salts of cheaper and less toxic halides as nucleophilic halogen sources. However, to address the issues associated with acyl chlorides (which are relatively unstable among carboxylic acid derivatives) and acyl fluorides (which are chemically stable but relatively expensive), as well as the contamination of the phenyl group in Xantphos in the product, we conceived a similar reaction using acid anhydrides. In this study, we further tested the compatibility and universality of Pd-catalyzed decarbonylative nucleophilic halogenation using acid anhydride substrates (Figure 1c). Notably, we report the successful synthesis of a series of aryl iodides, bromides, and chlorides in moderate to good yields. These reactions were particularly effective for substrates with electron-donating groups, such as methoxy groups, with significantly reduced catalytic poisoning, thus enhancing reaction efficiency.

## 2. Results and Discussion

Given the increasing demand for a cost-effective and user-friendly synthetic methodology for aryl iodides, we aimed to overcome the existing limitations through an innovative reaction design. As an initial approach, we selected 1-naphthoic anhydride (**1a**) as the substrate and sought to establish an optimized palladium catalytic system for decarbonylative nucleophilic iodination. Through systematic exploration of reaction conditions, we identified that a catalytic system comprising a bidentate ligand, Xantphos, with a large bite angle, and [PdCl(cinnamyl)]<sub>2</sub> exhibited the highest catalytic efficiency. Notably, employing lithium iodide—a relatively strong nucleophilic iodine source—in toluene at 100 °C for 24 h proved to be optimal. Further investigations into key reaction parameters, including ligands, catalyst precursors, iodide sources, and solvents, confirmed that under the optimized conditions, the desired decarbonylative iodinated product, 1-iodonaphthalene (**2a**), was obtained in an excellent 97% yield (Table 1, entry 1). Note that 0.194 mmol of **2a** is produced from 0.2 mmol of **1a**. In other words, not all of the substrate, acid anhydride **1a**, is converted into product **2a**; a portion is likely transformed into the lithium salt of the corresponding

aromatic carboxylic acid (*vide infra*). When alternative bidentate ligands with large bite angles, such as DPEphos and dtbpf, were used in place of Xantphos, a significant decrease in conversion was observed (entries 2 and 3). Similarly, monodentate phosphine ligands such as  $P(t\text{-Bu})_3$  and BrettPhos—both known to facilitate C–X bond reductive elimination [43–45,118,119]—were ineffective, resulting in little to no decarbonylative iodination (entries 4 and 5). These results suggest that bidentate phosphine ligands are more favorable for achieving efficient decarbonylative nucleophilic iodination than their monodentate counterparts. Next, we evaluated different palladium catalyst precursors. When  $\text{Pd}_2(\text{dba})_3$  was used, product **2a** was obtained in a moderate 68% yield, whereas  $\text{PdCl}_2$  proved to be an ineffective catalyst precursor (entries 6 and 7). Additionally, we explored whether  $\text{Ni}(\text{cod})_2$ —a nickel catalyst with properties similar to palladium—could serve as a viable alternative; however, this catalytic system was incompatible with the transformation (entry 8). Subsequent investigations revealed that the choice of iodine source significantly influenced the catalytic process. When sodium iodide (NaI) was used in place of lithium iodide (LiI), the expected reaction scarcely proceeded, likely due to the weaker nucleophilicity of NaI (entry 9). Additionally, changing the reaction solvent to THF or lowering the reaction temperature to 80 °C led to a considerable decrease in the yield of 1-iodonaphthalene, resulting in 30% and 55% yields, respectively (entries 10 and 11). Furthermore, we explored whether symmetrical acid anhydrides were necessary for the reaction. To evaluate this, a mixed anhydride, 1-naphthoic acid pivalic anhydride, was synthesized and investigated for reactivity. As a result, all substrate **1a** was completely consumed, but only 25% of the target product **2a** was obtained, and the expected byproduct,  $t\text{BuI}$ , was not detected. This result indicates that the presence of a symmetrical acid anhydride is essential for the present catalytic reaction (entry 12). Finally, control experiments confirmed that the reaction did not proceed at all in the absence of either the catalyst or ligand (entry 13). Based on these findings, the optimized reaction conditions were established as a combination of  $[\text{PdCl}(\text{cinnamyl})]_2$ /Xantphos, LiI, and toluene at 100 °C for 24 h. Further details on reaction condition optimization are provided in Tables S1–S6.

**Table 1.** Selected optimization data for the iodination of 1-naphthoic anhydride (**1a**).



**1a** (1.5 equiv) + **LiI**  $\xrightarrow[\text{toluene (0.2 M), 100 }^\circ\text{C, 24 h}]{[\text{PdCl(cinnamyl)}]_2 \text{ (3 mol \%), Xantphos (15 mol \%)}}$  **2a** + **3a**

Entry	Deviations from the Standard Conditions	<b>2a</b> (%) <sup>a</sup>	<b>3a</b> (%) <sup>a</sup>
1	None	97	<1
2	DPEphos instead of Xantphos	34	<1
3	dtbpf instead of Xantphos	37	<1
4	$P(t\text{-Bu})_3 \cdot \text{HBF}_4$ instead of Xantphos	<1	<1
5	BrettPhos instead of Xantphos	5	<1
6	$\text{Pd}_2(\text{dba})_3$ instead of $[\text{PdCl}(\text{cinnamyl})]_2$	68	<1
7	$\text{PdCl}_2$ instead of $[\text{PdCl}(\text{cinnamyl})]_2$	<1	<1
8	$\text{Ni}(\text{cod})_2$ instead of $[\text{PdCl}(\text{cinnamyl})]_2$	<1	<1
9	NaI instead of LiI	<5	<1
10	THF instead of toluene	30	<1
11	80 °C instead of 100 °C	55	<1
12	1-naphthoic pivalic anhydride instead of <b>1a</b>	25	<1
13	<i>w/o</i> $[\text{PdCl}(\text{cinnamyl})]_2$ or Xantphos	0	0

<sup>a</sup> Reaction conditions: **1a** (0.2 mmol, 1 equiv),  $[\text{PdCl}(\text{cinnamyl})]_2$  (3 mol %), Xantphos (15 mol %), LiI (1.5 equiv), toluene (0.2 M), 100 °C, 24 h. Yields were determined by  $^1\text{H}$  NMR using dibromomethane as an internal standard.



In the next stage, we investigated the compatibility of various substrates for decarbonylative iodination (Figure 2). Initially, several neutral anhydrides showed robust compatibility with the optimized reaction conditions, including 1-naphthoic anhydride (**1a**), benzoic anhydride (**1b**), and 2-naphthoic anhydride (**1c**), all of which afforded the corresponding decarbonylative nucleophilic iodination products—1-iodonaphthalene (**2a**), iodobenzene (**2b**), and 2-iodonaphthalene (**2c**)—in good to excellent yields. Next, we explored the influence of electronic effects on the substrates in this protocol. Specifically, we focused on the compatibility of anhydrides with electron-donating substituents, such as 3-methoxy-(**1d**) and 4-methoxy-(**1e**) benzoic anhydrides. However, the results revealed that only low yields of the desired products were obtained, likely due to catalyst poisoning. Consequently, we initiated an investigation into the reaction conditions for acid anhydrides with electron-donating groups. After a series of experiments using **1d** as the standard substrate, we found that slightly increasing the catalyst loading and using an open system improved the yield of nucleophilic iodination (see Table S9 for details). As a result, the corresponding 3-methoxyiodobenzene (**2d**) and 4-methoxyiodobenzene (**2e**) were obtained in yields of 71% and 32%, respectively. This improvement is primarily due to the removal of generated CO, which shifts the equilibrium toward product formation. In parallel, we also investigated the compatibility of other electron-donating substituents such as 4-*t*-Bu, 4-Ph, and 3-Ph groups. Fortunately, when we increased the reaction temperature, the decarbonylative transformation proceeded efficiently, yielding the corresponding iodinated products, 4-*tert*-butyl iodobenzene (**2f**), 4-iodobiphenyl (**2g**), and 3-iodobiphenyl (**2h**) in 60%, 49%, and 81% yields, respectively. Acid anhydrides with electron-donating substituents require more energy to facilitate thermodynamically unfavorable oxidative additions, which may have been enhanced under high-temperature conditions.

On the other hand, we investigated the effect of halogen substituents on this catalytic system. To our delight, highly reactive brominated **1i** and iodinated **1j** benzoic anhydrides were unexpectedly compatible with this reaction. These substrates produced the corresponding decarbonylative iodination products—4-bromoiodobenzene (**2i**) and 1,4-diiodobenzene (**2j**)—in moderate yields with good chemoselectivity. Additionally, even anhydrides with strong electron-withdrawing substituents, such as 4-CN and 4-CO<sub>2</sub>Me, did not interfere with the nucleophilic iodination process. The corresponding yields of 4-iodobenzonitrile (**2k**) and methyl 4-iodobenzoate (**2l**) were 82% and 43%, respectively. Subsequently, heteroaromatic anhydrides, such as benzofuran-2-carboxylic anhydride (**1m**), were also compatible with this decarbonylative transformation. However, the corresponding iodinated product **2m** was obtained in lower yields, likely due to the formation of the decarbonylative reduction product, benzofuran, as a side product. Finally, to highlight the potential application of this protocol in pharmaceutical engineering, we investigated derivatives of the pharmaceutical molecule, Probenecid, and found that **1n** could still yield the corresponding nucleophilic iodinated product **2n** in 57% yield.

Critically, we found that the developed Pd catalyst system can be extended to the construction of C–Br and C–Cl bonds by simply changing the halogenating agents under higher reaction temperatures due to the highly endothermic nature of the reductive elimination process of the C–X bond. The decarbonylative nucleophilic bromination produced the corresponding 1-bromonaphthalene (**4a**) in 89% yield. However, the chlorination process only afforded the corresponding 1-chloronaphthalene (**5a**) in 51% yield, even with 3 equiv of LiCl as the chloride source. Nevertheless, 41% of the starting material **1a** remained unreacted, likely due to the weak nucleophilicity and low solubility of LiCl.

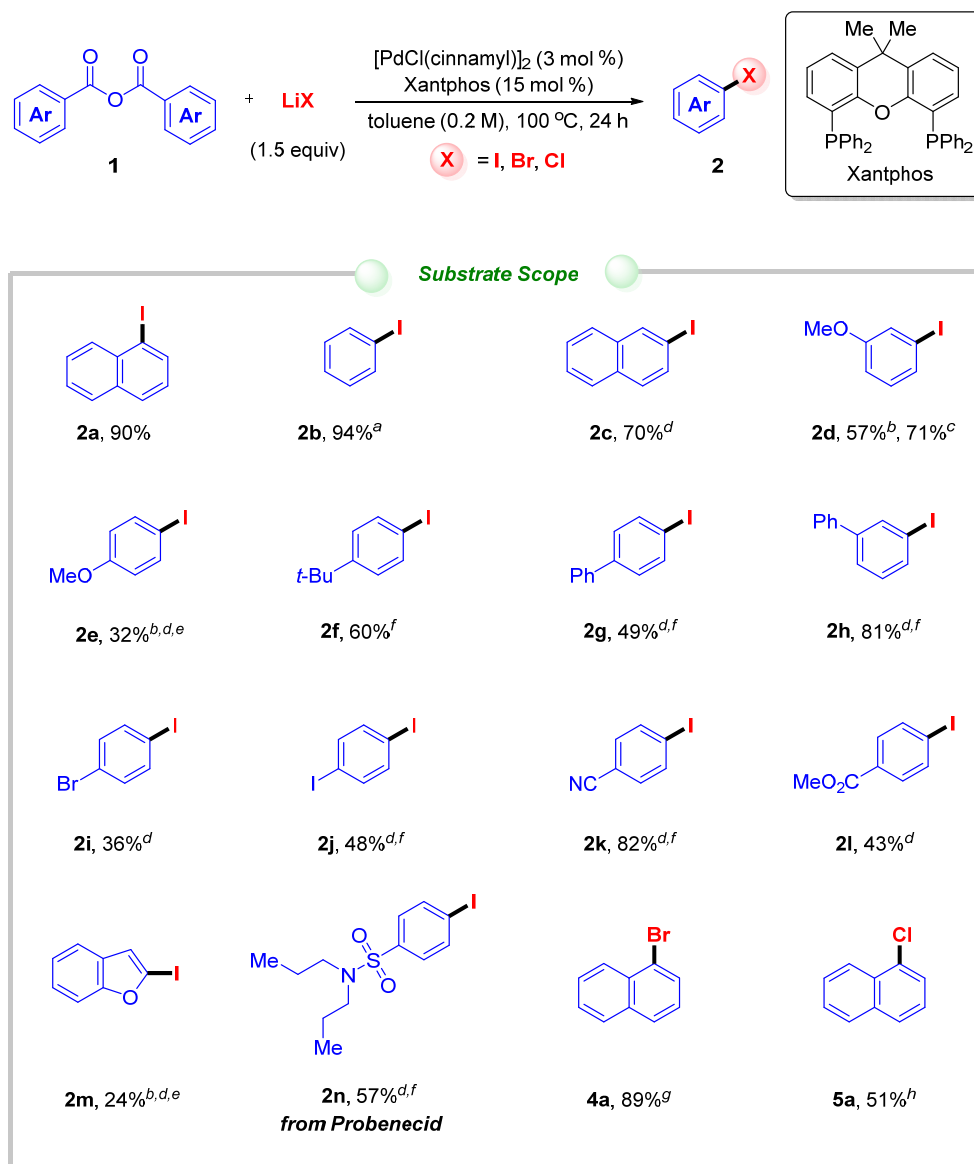


**Figure 2.** Substrate scope for decarbonylative nucleophilic halogenation of acid anhydrides **1**. Reaction conditions: Acid anhydrides **1** (0.2 mmol, 1 equiv),  $[\text{PdCl}(\text{cinnamyl})]_2$  (3 mol %), Xantphos (15 mol %), LiI (1.5 equiv), toluene (0.2 M), 100 °C, 24 h. Isolated yields are shown unless otherwise indicated. <sup>a</sup> GC yield was determined using *n*-dodecane as an internal standard. <sup>b</sup> open system; toluene (0.1 M). <sup>c</sup> NMR yield was determined by  $^1\text{H}$  NMR, using dibromomethane as an internal standard. <sup>d</sup>  $[\text{PdCl}(\text{cinnamyl})]_2$  (3.5 mol %), Xantphos (17.5 mol %). <sup>e</sup> 120 °C, 12 h. <sup>f</sup> 140 °C, 12 h. <sup>g</sup> 160 °C, LiBr (0.3 mmol, 1.5 equiv) <sup>h</sup> 160 °C, LiCl (0.6 mmol, 3 equiv).

We conducted mechanistic studies based on our hypotheses to gain a deeper understanding of the catalytic transformation. First, we performed time-course studies and monitored the  $^{31}\text{P}\{^1\text{H}\}$  NMR spectra for the stoichiometric Pd-mediated decarbonylative nucleophilic iodination process to identify potential intermediates (see Figure S4 for details). Initially, when  $\text{Pd}(\text{dba})_2$  and Xantphos were mixed, the previously reported  $(\text{Xantphos})_2\text{Pd}$  (two broad singlets at  $-0.1$  and  $3.1$  ppm) and  $(\text{Xantphos})\text{Pd}(\text{dba})$  (two doublets at  $8.1$  and  $10.2$  ppm) were observed [116,120]. Upon the addition of benzoic anhydride (**1b**), the mixture was monitored to determine whether the expected oxidative addition had occurred. However, no significant changes were observed even when the temperature was increased from room temperature to 50 °C. Subsequently, upon adding LiI into the reaction mixture, the oxidative adduct *trans*-(Xantphos)Pd(II)(COPh)I [121] was detected at room

temperature after 1 h. As the temperature was further increased (from 50 °C to 75 °C), the decarbonylative complex, *trans*-(Xantphos)Pd(II)(Ph)I [116,121], was detected via the carbonyl de-insertion process. Based on the identification of these two key intermediates, we proposed a unimolecular fragment coupling (UFC) mechanism [122]. The core of this mechanism involves the in situ formation of acyl iodide, a transient intermediate, via nucleophilic substitution of the acid anhydride **1** with LiI. Crucially, as we have previously discussed [117], the key to the success of this pathway lies in the rate of acyl iodide formation, which must occur slowly and gradually to ensure efficient conversion and avoid catalyst poisoning. Therefore, we monitored the reaction using <sup>1</sup>H NMR spectroscopy at room temperature, 50 °C, and 100 °C to investigate whether acyl iodide forms from the mixture of 1-naphthoic anhydride (**1a**) and LiI (Tables S10–S12). However, no acyl iodide (**6**) was detected at room temperature, and only trace amounts were observed at 50 °C (see Tables S10 and S11 for details). At 100 °C, only 4% of 1-naphthoyl iodide (**6**) was formed after 1 h, and the yield remained low at 47% even after 24 h. Additionally, a white solid, identified as lithium 1-naphthoate (**7**), precipitated due to its low solubility in toluene (Figure 3 and Table S12 for details).

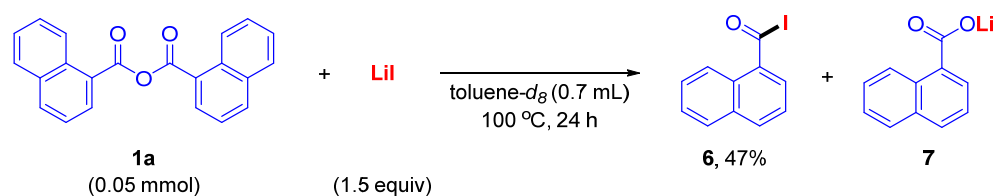


**Figure 3.** Generation of 1-naphthoyl iodide (**6**).

However, this result contradicts the experimental observation that no reaction occurred when benzoic anhydride (**1b**) was added to the Pd(dba)<sub>2</sub>/Xantphos mixture. Yet, upon subsequent addition of LiI, the *trans*-(Xantphos)Pd(II)(COPh)I signal was detected even at room temperature. To investigate further, we added LiI to the Pd(dba)<sub>2</sub>/Xantphos mixture and recorded the <sup>31</sup>P{<sup>1</sup>H} NMR spectrum (Figure S5). After 1 h at room temperature, the signal for (Xantphos)<sub>2</sub>Pd remained largely unchanged, while the signal assignable to (Xantphos)Pd(dba) disappeared, and two new singlets at 7.4 and 11.0 ppm emerged. Furthermore, when benzoic anhydride (**1b**) was added to this mixture, the *trans*-(Xantphos)Pd(II)(COPh)I signal appeared at room temperature after 1 h. These results suggest that LiI does not react with acid anhydride **1** at room temperature without the catalyst, but in the presence of the catalyst, an apparent oxidative addition of the acyl iodide occurs.

Based on a brief mechanistic study, we propose two possible mechanisms (Figure 4). The first mechanism follows a decarbonylative unimolecular fragment coupling (UFC) pathway (Path A). Initially, LiI-mediated nucleophilic substitution of the acid anhydride **1** generates acyl halide intermediate **B**. This acyl halide then undergoes oxidative addition with the active Pd(0) complex **A**, forming the acyl-Pd-X intermediate **C**. Subsequent carbonyl de-insertion and reductive elimination generate the desired decarbonylative halogenated product **2** while regenerating the active Pd(0) catalyst **A**. In an alternative mechanism (Path B), the palladium catalyst is converted into the anionic palladate complex **E** in the presence of lithium halide [122]. This anionic complex **E**, being electron-rich, facilitates the facile oxidative addition of acid anhydride **1**, leading to the formation of the common intermediate **C**. The subsequent steps proceed similarly to Path A.



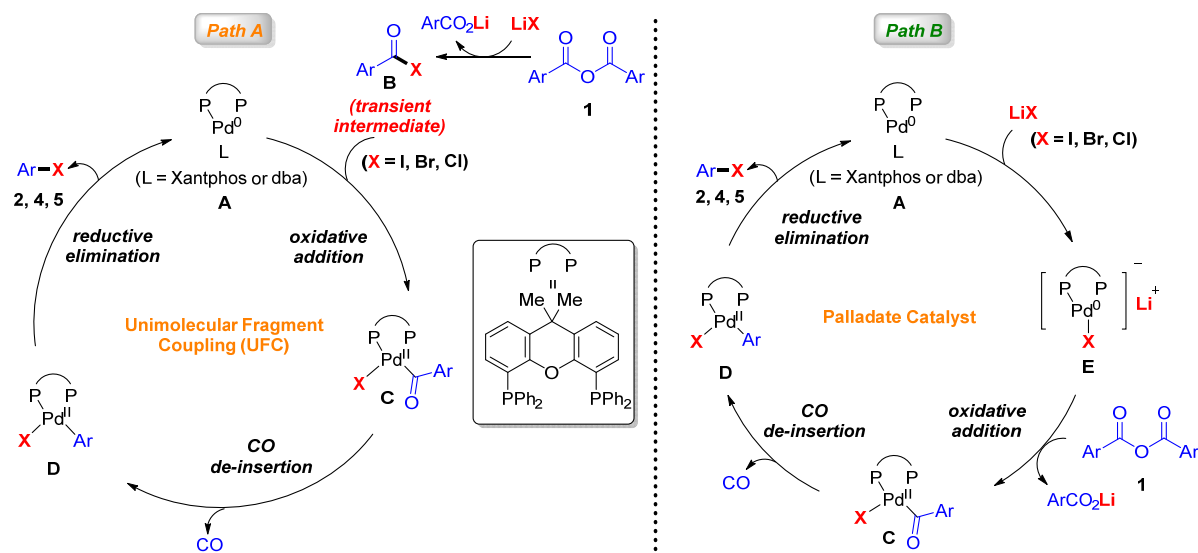


Figure 4. Two plausible mechanisms.

### 3. Materials and Methods

#### 3.1. General

Unless otherwise stated, all reactions were conducted under an N<sub>2</sub> atmosphere using standard Schlenk techniques or a glovebox. Solvents used as eluents for routine operations, as well as dehydrated solvents, were purchased from commercial suppliers and used without further purification. All glassware was dried in an oven at 130 °C and evacuated before use. Thin-layer chromatography (TLC) analyses were performed using Merck (Boston, MA, USA) precoated silica gel 60 F<sub>254</sub> plates (0.25 mm). Silica gel column chromatography was carried out with Silica Gel 60 N (spherical, neutral, 40–100 µm) from Kanto Chemicals Co., Ltd. (Tokyo, Japan). NMR spectra (<sup>1</sup>H, <sup>13</sup>C{<sup>1</sup>H}, and <sup>31</sup>P{<sup>1</sup>H}) were recorded on Mercury-400 (400 MHz) or Mercury-600 (600 MHz) spectrometers. Chemical shifts (δ) are reported in parts per million (ppm) relative to CDCl<sub>3</sub> at 7.26 ppm for <sup>1</sup>H and 77.16 ppm for <sup>13</sup>C{<sup>1</sup>H}, respectively. The <sup>31</sup>P{<sup>1</sup>H} NMR spectra were referenced using H<sub>3</sub>PO<sub>4</sub> (δ = 0.00 ppm) as an external standard. GC yields were determined by analyzing the crude reaction mixture using *n*-dodecane as an internal standard on a Shimadzu GC-14A gas chromatograph (Kyoto, Japan) equipped with a flame ionization detector. A Shimadzu Capillary Column (CBP1-M25-025) and a Shimadzu C-R6A Chromatopac integrator were used for analysis. Infrared spectra were recorded on a Shimadzu IR Prestige-21 spectrophotometer. Elemental analyses were performed using a PerkinElmer (Springfield, IL, USA) 2400 CHN elemental analyzer at Okayama University. High-resolution mass spectra (HRMS) were obtained in electron ionization (EI) mode on a JEOL JMS-700 mass spectrometer (Peabody, MA, USA).

Unless specified otherwise, materials obtained from commercial suppliers were used without further purification. Palladium(II)( $\pi$ -cinnamyl) chloride dimer ([PdCl(cinnamyl)]<sub>2</sub>) (purity > 97%) was purchased from Tokyo Chemical Industry Co., Ltd. (Tokyo, Japan) and Sigma-Aldrich Co. LLC. (St. Louis, MO, USA). 4,5-Bis(diphenylphosphino)-9,9-dimethylxanthene (Xantphos) (purity > 98%) was purchased from Tokyo Chemical Industry Co., Ltd. Lithium iodide (purity > 97%) was purchased from FUJIFILM Co., Ltd. (Ebina-shi, Japan). Lithium bromide (purity > 99%) and lithium chloride (purity > 98%) were purchased from Tokyo Chemical Industry Co., Ltd. Toluene (super dehydrated) was purchased from FUJIFILM Co., Ltd. Benzoic anhydride (**1b**) (purity > 97%) was purchased from Tokyo Chemical Industry Co., Ltd.

### 3.2. Experimental Procedure

The synthetic methods and procedures for all anhydrides are provided in Procedures A, B, and C in the Supporting Information, while the main text focuses on the experimental procedures for decarbonylative nucleophilic halogenation.

#### 3.2.1. Representative Procedure for Decarbonylative Iodination of Acid Anhydrides **1** (Procedure D)

An oven-dried 5-mL microwave vial equipped with a magnetic stirring bar was charged with  $[\text{PdCl}(\text{cinnamyl})]_2$  (3–3.5 mol %, 6–7  $\mu\text{mol}$ , 3.1–3.6 mg), Xantphos (15–17.5 mol %, 0.03–0.035 mmol, 17.4–20.3 mg), and acid anhydrides **1** (0.2 mmol, 1 equiv) under ambient air. In a nitrogen-filled glovebox, lithium iodide (0.3 mmol, 1.5 equiv, 40.2 mg) and anhydrous toluene (1 mL, 0.2 M) were added. The vial was securely sealed and heated in a preheated block at 100–140 °C for 12–24 h with continuous stirring. After cooling to room temperature, the reaction mixture was purified by silica gel column chromatography using ethyl acetate or dichloromethane/hexane as the eluent to obtain the desired product **2**. Yields of the volatile product **2b** were determined by GC analysis of the reaction mixture, using *n*-dodecane as an internal standard.

#### 3.2.2. Representative Procedure for Decarbonylative Iodination of Acid Anhydrides **1** (Procedure E) (Open System)

An oven-dried 5-mL microwave vial equipped with a magnetic stirring bar was loaded with  $[\text{PdCl}(\text{cinnamyl})]_2$  (3.5 mol %, 7  $\mu\text{mol}$ , 3.6 mg), Xantphos (17.5 mol %, 0.035 mmol, 20.3 mg), and acid anhydrides **1** (0.2 mmol, 1 equiv) under ambient air. Lithium iodide (0.3 mmol, 1.5 equiv, 40.2 mg) and anhydrous toluene (2 mL, 0.1 M) were added to a nitrogen-filled glovebox. The vial was securely sealed, and the septum was pierced with a needle for pressure equilibration (the appearance of the reaction set-up is shown in the Supporting Information). The vial was then placed in a preheated heating block at 100–120 °C and stirred for 12 h. After cooling to room temperature, the reaction mixture was purified by silica gel column chromatography using a dichloromethane/hexane mixture or pure hexane as the eluent, yielding the desired products.

#### 3.2.3. Representative Procedure for Decarbonylative Bromination of 1-Naphthoic Anhydrides **1a** (Procedure F)

An oven-dried 5-mL microwave vial equipped with a magnetic stirring bar was charged with  $[\text{PdCl}(\text{cinnamyl})]_2$  (3 mol %, 6  $\mu\text{mol}$ , 3.1 mg), Xantphos (15 mol %, 0.03 mmol, 17.4 mg), and 1-naphthoic anhydride **1a** (0.2 mmol, 1 equiv, 65.3 mg) under ambient air. Lithium bromide (0.3 mmol, 1.5 equiv, 26.1 mg) and anhydrous toluene (1 mL, 0.2 M) were introduced in a nitrogen-filled glovebox. The vial was securely sealed and heated in a preheated block at 160 °C for 24 h with continuous stirring. **Safety Note:** The reaction must be conducted in a fume hood, as the temperature exceeds toluene's boiling point, and carbon monoxide (CO) is generated. There is a potential risk of the reaction cap detaching due to pressure buildup. After cooling to room temperature, the reaction mixture was purified by silica gel column chromatography using a suitable eluent to isolate the desired product **4a**.

#### 3.2.4. Representative Procedure for Decarbonylative Chlorination of 1-Naphthoic Anhydrides **1a** (Procedure G)

An oven-dried 5-mL microwave vial equipped with a magnetic stirring bar was charged with  $[\text{PdCl}(\text{cinnamyl})]_2$  (3 mol %, 6  $\mu\text{mol}$ , 3.1 mg), Xantphos (15 mol %, 0.03 mmol, 17.4 mg), and 1-naphthoic anhydride **1a** (0.2 mmol, 1 equiv, 65.3 mg) under ambient air. Lithium chloride (0.6 mmol, 3 equiv, 25.4 mg) and anhydrous toluene (1 mL, 0.2 M) were

added inside a nitrogen-filled glovebox. The vial was securely sealed and heated in a preheated block at 160 °C for 24 h with continuous stirring. **Safety Note:** The reaction must be conducted in a fume hood. Due to the high reaction temperature, which exceeds toluene's boiling point, and the generation of CO gas, there is a potential risk of the reaction cap detaching due to pressure buildup. After cooling the reaction mixture to room temperature, it was purified by silica gel column chromatography using hexane as the eluent to isolate the desired product **5a**.

### 3.3. Characterization Data of Products

**1-Iodonaphthalene (2a)** [117]. Prepared according to procedure D as a yellow oil.  $R_f$  = 0.60 (hexane). The isolated yield was 90% (45.9 mg) from **1a**.  $^1\text{H}$  NMR (600 MHz,  $\text{CDCl}_3$ ):  $\delta$  8.14–8.10 (m, 2H), 7.85 (d,  $J$  = 8.2 Hz, 1H), 7.78 (d,  $J$  = 7.8 Hz, 1H), 7.60 (t,  $J$  = 7.6 Hz, 1H), 7.53 (t,  $J$  = 7.5 Hz, 1H), 7.19 (t,  $J$  = 7.8 Hz, 1H);  $^{13}\text{C}\{^1\text{H}\}$  NMR (151 MHz,  $\text{CDCl}_3$ ):  $\delta$  137.5, 134.5, 134.2, 132.2, 129.1, 128.7, 127.8, 127.0, 126.8, 99.7.

**2-Iodonaphthalene (2c)** [117]. Prepared according to procedure D as a white solid.  $R_f$  = 0.60 (hexane). The isolated yield was 70% (35.4 mg) from **1c**.  $^1\text{H}$  NMR (400 MHz,  $\text{CDCl}_3$ ):  $\delta$  8.24–8.24 (m, 1H), 7.81–7.78 (m, 1H), 7.73–7.71 (m, 2H), 7.58 (d,  $J$  = 8.6 Hz, 1H), 7.50 (dt,  $J$  = 6.3, 3.5 Hz, 2H);  $^{13}\text{C}\{^1\text{H}\}$  NMR (101 MHz,  $\text{CDCl}_3$ ):  $\delta$  136.8, 135.1, 134.5, 132.2, 129.6, 128.0, 126.9, 126.8, 126.6, 91.6.

**1-Iodo-3-methoxybenzene (2d)** [117]. Prepared according to procedure E as a colorless oil.  $R_f$  = 0.40 (DCM/hexane = 1/10). The isolated yield was 57% (26.8 mg) from **1d**.  $^1\text{H}$  NMR (600 MHz,  $\text{CDCl}_3$ ):  $\delta$  7.28 (ddt,  $J$  = 7.8, 1.8, 0.9 Hz, 1H), 7.25 (dt,  $J$  = 2.5, 1.2 Hz, 1H), 7.00 (t,  $J$  = 8.1 Hz, 1H), 6.87 (dd,  $J$  = 8.4, 2.5 Hz, 1H), 3.78 (s, 3H);  $^{13}\text{C}\{^1\text{H}\}$  NMR (151 MHz,  $\text{CDCl}_3$ ):  $\delta$  160.3, 130.9, 130.0, 123.1, 113.9, 94.5, 55.5.

**1-Iodo-4-methoxybenzene (2e)** [117]. Prepared according to procedure E as a colorless oil.  $R_f$  = 0.40 (DCM/hexane = 1/10). The isolated yield was 32% (15.2 mg) from **1e**.  $^1\text{H}$  NMR (600 MHz,  $\text{CDCl}_3$ ):  $\delta$  7.57–7.54 (m, 2H), 6.70–6.67 (m, 2H), 3.78 (s, 3H);  $^{13}\text{C}\{^1\text{H}\}$  NMR (151 MHz,  $\text{CDCl}_3$ ): 159.6, 138.3, 116.5, 82.8, 55.4.

**1-(tert-butyl)-4-iodobenzene (2f)** [117]. Prepared according to procedure D as a white solid.  $R_f$  = 0.80 (hexane). The isolated yield was 60% (31.1 mg) from **1f**.  $^1\text{H}$  NMR (400 MHz,  $\text{CDCl}_3$ ):  $\delta$  7.64–7.60 (m, 2H), 7.17–7.13 (m, 2H), 1.30 (s, 9H);  $^{13}\text{C}\{^1\text{H}\}$  NMR (101 MHz,  $\text{CDCl}_3$ ):  $\delta$  151.0, 137.2, 127.7, 90.8, 34.7, 31.3.

**4-Iodo-1,1'-biphenyl (2g)** [117]. Prepared according to procedure D as a white solid.  $R_f$  = 0.55 (hexane). The isolated yield was 49% (27.6 mg) from **1g**.  $^1\text{H}$  NMR (600 MHz,  $\text{CDCl}_3$ ):  $\delta$  7.78–7.76 (m, 2H), 7.57–7.55 (m, 2H), 7.45 (t,  $J$  = 7.6 Hz, 2H), 7.39–7.36 (m, 1H), 7.35–7.33 (m, 2H);  $^{13}\text{C}\{^1\text{H}\}$  NMR (151 MHz,  $\text{CDCl}_3$ ):  $\delta$  140.9, 140.2, 138.0, 129.1, 129.0, 127.8, 127.0, 93.2.

**3-Iodo-1,1'-biphenyl (2h)** [117]. Prepared according to procedure D as a colorless oil.  $R_f$  = 0.55 (hexane). The isolated yield was 81% (45.1 mg) from **1h**.  $^1\text{H}$  NMR (600 MHz,  $\text{CDCl}_3$ ):  $\delta$  7.95 (t,  $J$  = 1.7 Hz, 1H), 7.68 (ddd,  $J$  = 7.9, 1.8, 1.0 Hz, 1H), 7.56–7.54 (m, 3H), 7.46–7.43 (m, 2H), 7.39–7.36 (m, 1H), 7.18 (t,  $J$  = 7.8 Hz, 1H);  $^{13}\text{C}\{^1\text{H}\}$  NMR (151 MHz,  $\text{CDCl}_3$ ):  $\delta$  143.6, 139.8, 136.32, 136.28, 130.5, 129.0, 128.0, 127.2, 126.5, 94.9.

**1-Bromo-4-iodobenzene (2i)** [117]. Prepared according to procedure D as a white solid.  $R_f$  = 0.80 (hexane). The isolated yield was 36% (20.3 mg) from **1i**.  $^1\text{H}$  NMR (600 MHz,  $\text{CDCl}_3$ ):  $\delta$  7.56–7.53 (m, 2H), 7.24–7.22 (m, 2H);  $^{13}\text{C}\{^1\text{H}\}$  NMR (151 MHz,  $\text{CDCl}_3$ ):  $\delta$  139.2, 133.6, 122.3, 92.2.

**1,4-Diiodobenzene (2j)** [117]. Prepared according to procedure D as a white solid.  $R_f$  = 0.80 (hexane). The isolated yield was 48% (31.1 mg) from **1j**.  $^1\text{H}$  NMR (600 MHz,  $\text{CDCl}_3$ ):  $\delta$  7.41 (s, 4H);  $^{13}\text{C}\{^1\text{H}\}$  NMR (151 MHz,  $\text{CDCl}_3$ ):  $\delta$  139.5, 93.5.

**4-Iodobenzonitrile (2k)** [117]. Prepared according to procedure D as a white solid.  $R_f$  = 0.30 (DCM/hexane = 1/1). The isolated yield was 82% (37.3 mg) from **1k**.  $^1\text{H}$  NMR (600 MHz,  $\text{CDCl}_3$ ):  $\delta$  7.86–7.83 (m, 2H), 7.37–7.35 (m, 2H);  $^{13}\text{C}\{^1\text{H}\}$  NMR (151 MHz,  $\text{CDCl}_3$ ):  $\delta$  138.6, 133.3, 118.3, 111.9, 100.4.

**Methyl 4-Iodobenzoate (2l)** [117]. Prepared according to procedure D as a white solid.  $R_f$  = 0.40 (DCM/hexane = 1/1). The isolated yield was 43% (22.6 mg) from **1l**.  $^1\text{H}$  NMR (600 MHz,  $\text{CDCl}_3$ ):  $\delta$  7.81–7.79 (m, 2H), 7.75–7.73 (m, 2H), 3.91 (s, 3H);  $^{13}\text{C}\{^1\text{H}\}$  NMR (151 MHz,  $\text{CDCl}_3$ ):  $\delta$  166.7, 137.9, 131.2, 129.7, 100.9, 52.4.

**2-Iodobenzofuran (2m)** [117]. Prepared according to procedure E as a colorless oil.  $R_f$  = 0.60 (hexane). The isolated yield was 24% (11.8 mg) from **1m**.  $^1\text{H}$  NMR (600 MHz,  $\text{CDCl}_3$ ):  $\delta$  7.52–7.50 (m, 1H), 7.48–7.46 (m, 1H), 7.24–7.19 (m, 2H), 6.96 (s, 1H);  $^{13}\text{C}\{^1\text{H}\}$  NMR (151 MHz,  $\text{CDCl}_3$ ):  $\delta$  158.3, 129.3, 124.4, 123.3, 119.8, 117.4, 111.0, 96.0.

**4-Iodo-N,N-dipropylbenzenesulfonamide (2n)** [117]. Prepared according to procedure D as a white solid.  $R_f$  = 0.40 (DCM/hexane = 2/1). The isolated yield was 57% (41.8 mg) from **1n**.  $^1\text{H}$  NMR (400 MHz,  $\text{CDCl}_3$ ):  $\delta$  7.86–7.82 (m, 2H), 7.52–7.49 (m, 2H), 3.07–3.04 (m, 4H), 1.54 (dq,  $J$  = 14.9, 7.4 Hz, 4H), 0.86 (t,  $J$  = 7.4 Hz, 6H);  $^{13}\text{C}\{^1\text{H}\}$  NMR (101 MHz,  $\text{CDCl}_3$ ):  $\delta$  140.0, 138.3, 128.6, 99.5, 50.1, 22.1, 11.3.

**1-Bromonaphthalene (4a)** [117]. Prepared according to procedure F as a colorless oil.  $R_f$  = 0.60 (hexane). The isolated yield was 89% (36.7 mg) from **1a**.  $^1\text{H}$  NMR (400 MHz,  $\text{CDCl}_3$ ):  $\delta$  8.28 (d,  $J$  = 8.4 Hz, 1H), 7.87–7.80 (m, 3H), 7.62 (ddd,  $J$  = 8.5, 6.9, 1.5 Hz, 1H), 7.56 (td,  $J$  = 7.5, 6.8, 1.4 Hz, 1H), 7.34 (t,  $J$  = 7.8 Hz, 1H);  $^{13}\text{C}\{^1\text{H}\}$  NMR (151 MHz,  $\text{CDCl}_3$ ):  $\delta$  134.7, 132.1, 130.0, 128.4, 128.0, 127.4, 127.2, 126.8, 126.3, 122.9.

**1-Chloronaphthalene (5a)** [117]. Prepared according to procedure G as a colorless oil.  $R_f$  = 0.55 (hexane). The isolated yield was 51% (16.5 mg) from **1a**.  $^1\text{H}$  NMR (400 MHz,  $\text{CDCl}_3$ ):  $\delta$  8.33–8.30 (m, 1H), 7.88 (d,  $J$  = 8.0 Hz, 1H), 7.79 (d,  $J$  = 8.2 Hz, 1H), 7.65–7.55 (m, 3H), 7.42–7.38 (m, 1H);  $^{13}\text{C}\{^1\text{H}\}$  NMR (101 MHz,  $\text{CDCl}_3$ ):  $\delta$  134.7, 132.0, 130.9, 128.3, 127.3, 127.2, 126.8, 126.3, 125.8, 124.5.

## 4. Conclusions

In summary, we have developed an efficient palladium-catalyzed decarbonylative nucleophilic halogenation strategy, particularly for the iodination of aromatic acid anhydrides. This transformation leverages the unique metastable properties of acid anhydrides to circumvent the instability of acyl chlorides and the high cost of acyl fluorides, demonstrating significant potential in synthetic organic chemistry and related fields. Moreover, the sterically bulky and *trans*-coordinated nature of the Xantphos ligand has once again proven to be a highly versatile and compatible ligand for thermodynamically and kinetically challenging processes, such as Pd(II)-mediated reductive elimination of C–X bonds. As a result, we have successfully achieved a series of decarbonylative nucleophilic halogenation reactions, including chlorination, bromination, and iodination, via Pd(II)-catalyzed reductive elimination of C–I, C–Br, and C–Cl bonds, respectively. For substrates bearing electron-donating substituents, such as methoxy groups, reaction efficiency was enhanced by conducting the reaction in an open system. Mechanistic studies suggest a plausible decarbonylative unimolecular fragment coupling (UFC) pathway or an alternative route involving an anionic palladate complex. The unique properties of acid anhydrides played a crucial role in enhancing catalytic performance by modulating the reactivity of iodide salts, thereby minimizing side reactions and improving overall efficiency. These findings provide valuable

insights and a strong foundation for future advancements in transition-metal-catalyzed transformations.

**Supplementary Materials:** The following supporting information can be downloaded at: <https://www.mdpi.com/article/10.3390/catal15020191/s1>. Detailed screening of reaction conditions for decarbonylative halogenation is presented in Tables S1–S9. The experimental results monitoring the formation of acyl iodides at various temperatures are presented in Tables S10–S12. The structures of the acid anhydrides examined in this study are shown in Figures S1 and S2, while the structures of the ligands are depicted in Figure S3. The  $^{31}\text{P}\{^1\text{H}\}$  NMR spectra recorded for the mechanistic studies are provided in Figures S4 and S5. Additionally, the synthesis and characterization of acid anhydrides, along with the  $^1\text{H}$  NMR and  $^{13}\text{C}\{^1\text{H}\}$  NMR spectra of all the starting materials and final products, are provided in the Supporting Information. Refs. [92,123–130] are cited in the Supplementary Materials.

**Author Contributions:** T.T. developed the reactions and wrote the manuscript; S.U. and W.Y. prepared the starting materials, expanded the substrate scope, and conducted the mechanistic studies; Y.N. supervised the project and revised the manuscript. All authors have read and agreed to the published version of the manuscript.

**Funding:** This research received no external funding.

**Data Availability Statement:** The original contributions presented in this study are included in the article Supplementary Material. Further inquiries can be directed to the corresponding authors.

**Acknowledgments:** We gratefully thank Megumi Kosaka and Motonari Kobayashi (Department of Instrumental Analysis, Advanced Science Research Center, Okayama University) for performing elemental analyses and the SC-NMR Laboratory (Okayama University) for the NMR spectral measurements. We gratefully thank Masaya Sawamura of Hokkaido University for the insightful discussions. T.T. (student ID: 202208050057) and W.Y. (student ID: 202306870013) are grateful for financial support from the China Scholarship Council (CSC).

**Conflicts of Interest:** The authors declare no conflicts of interest.

## References

1. Hernandez, M.Z.; Cavalcanti, S.M.T.; Moreira, D.R.M.; de Azevedo, W.F., Jr.; Leite, A.C.L. Halogen Atoms in the Modern Medicinal Chemistry: Hints for the Drug Design. *Curr. Drug Targets* **2010**, *11*, 303–314. [CrossRef]
2. Wilcken, R.; Zimmermann, M.O.; Lange, A.; Joerger, A.C.; Boeckler, F.M. Principles and Applications of Halogen Bonding in Medicinal Chemistry and Chemical Biology. *J. Med. Chem.* **2013**, *56*, 1363–1388. [CrossRef]
3. Tang, M.L.; Bao, Z. Halogenated Materials as Organic Semiconductors. *Chem. Mater.* **2011**, *23*, 446–455. [CrossRef]
4. Gribble, G.W. Naturally Occurring Organohalogen Compounds. *Acc. Chem. Res.* **1998**, *31*, 141–152. [CrossRef]
5. Gribble, G.W. Structure and Biosynthesis of Halogenated Alkaloids. In *Modern Alkaloids: Structure, Isolation, Synthesis, and Biology*; Fattorusso, E., Tagliatella-Scafati, O., Eds.; Wiley-VCH: Weinheim, Germany, 2007.
6. Jeschke, P. The Unique Role of Halogen Substituents in the Design of Modern Crop Protection Compounds. In *Modern Methods in Crop Protection Research*; Jeschke, P., Krämer, W., Schirmer, U., Witschel, M., Eds.; Wiley-VCH: Weinheim, Germany, 2012.
7. Beale, T.M.; Chudzinski, M.G.; Sarwar, M.G.; Taylor, M.S. Halogen bonding in solution: Thermodynamics and applications. *Chem. Soc. Rev.* **2013**, *42*, 1667–1680. [CrossRef]
8. Stille, J.K.; Lau, K.S.Y. Mechanisms of Oxidative Addition of Organic Halides to Group 8 Transition-Metal Complexes. *Acc. Chem. Res.* **1977**, *10*, 434–442. [CrossRef]
9. Labinger, J.A. Tutorial on Oxidative Addition. *Organometallics* **2015**, *34*, 4784–4795. [CrossRef]
10. Rio, J.; Liang, H.; Perrin, M.-E.L.; Perego, L.A.; Grimaud, L.; Payard, P.-A. We Already Know Everything about Oxidative Addition to Pd(0): Do We? *ACS Catal.* **2023**, *13*, 11399–11421. [CrossRef]
11. Kvasovs, N.; Gevorgyan, V. Contemporary methods for generation of aryl radicals. *Chem. Soc. Rev.* **2021**, *50*, 2244–2259. [CrossRef]
12. Ghosh, I.; Marzo, L.; Das, A.; Shaikh, R.; König, B. Visible Light Mediated Photoredox Catalytic Arylation Reactions. *Acc. Chem. Res.* **2016**, *49*, 1566–1577. [CrossRef]
13. Pan, Q.; Ping, Y.; Kong, W. Nickel-Catalyzed Ligand-Controlled Selective Reductive Cyclization/Cross-Couplings. *Acc. Chem. Res.* **2023**, *56*, 515–535. [CrossRef]
14. Li, Y.; Hari, D.P.; Vita, M.V.; Waser, J. Cyclic Hypervalent Iodine Reagents for Atom-Transfer Reactions: Beyond Trifluoromethylation. *Angew. Chem. Int. Ed.* **2016**, *55*, 4436–4454, *Angew. Chem.* **2016**, *128*, 4512–4531. [CrossRef]



15. Brand, J.P.; Waser, J. Electrophilic alkynylation: The dark side of acetylene chemistry. *Chem. Soc. Rev.* **2012**, *41*, 4165–4179. [[CrossRef](#)]
16. Charpentier, J.; Früh, N.; Togni, A. Electrophilic Trifluoromethylation by Use of Hypervalent Iodine Reagents. *Chem. Rev.* **2015**, *115*, 650–682. [[CrossRef](#)]
17. Wang, X.; Studer, A. Iodine(III) Reagents in Radical Chemistry. *Acc. Chem. Res.* **2017**, *50*, 1712–1724. [[CrossRef](#)]
18. Cui, B.; Jia, S.; Tokunaga, E.; Shibata, N. Defluorosilylation of fluoroarenes and fluoroalkanes. *Nat. Commun.* **2018**, *9*, 4393. [[CrossRef](#)] [[PubMed](#)]
19. Gooßen, L.J.; Rodríguez, N.; Gooßen, K. Carboxylic Acids as Substrates in Homogeneous Catalysis. *Angew. Chem. Int. Ed.* **2008**, *47*, 3100–3120; *Angew. Chem.* **2008**, *120*, 3144–3164. [[CrossRef](#)]
20. Dzik, W.I.; Lange, P.P.; Gooßen, L.J. Carboxylates as sources of carbon nucleophiles and electrophiles: Comparison of decarboxylative and decarbonylative pathways. *Chem. Sci.* **2012**, *3*, 2671–2678. [[CrossRef](#)]
21. Borodine, A. Ueber Bromvaleriansäure Und Brombutersäure. *Liebigs Ann.* **1861**, *119*, 121–123. [[CrossRef](#)]
22. Hunsdiecker, H.; Hunsdiecker, C. Über den Abbau der Salze aliphatischer Säuren durch Brom. *Ber. Dtsch. Chem. Ges. B* **1942**, *75*, 291–297. [[CrossRef](#)]
23. Hunsdiecker, H.; Hunsdiecker, C.; Vogt, E. Method of Manufacturing Organic Chlorine and Bromine derivatives. U.S. Patent 2176181, 17 October 1939.
24. Varenikov, A.; Shapiro, E.; Gandelman, M. Decarboxylative Halogenation of Organic Compounds. *Chem. Rev.* **2021**, *121*, 412–484. [[CrossRef](#)] [[PubMed](#)]
25. Cornella, J.; Rosillo-Lopez, M.; Larrosa, I. A Novel Mode of Reactivity for Gold(I): The Decarboxylative Activation of (Hetero) Aromatic Carboxylic Acids. *Adv. Synth. Catal.* **2011**, *353*, 1359–1366. [[CrossRef](#)]
26. Cristol, S.; Firth, W., Jr. A Convenient Synthesis of Alkyl Halides from Carboxylic Acids. *J. Org. Chem.* **1961**, *26*, 280. [[CrossRef](#)]
27. Zhan, K.; Li, Y. Microwave-Assisted Silver-Catalyzed Protodecarboxylation and Decarboxylative Iodination of Aromatic Carboxylic Acids. *Catalysts* **2017**, *7*, 314. [[CrossRef](#)]
28. Hazarika, D.; Phukan, P. TsNBr<sub>2</sub> promoted decarboxylative bromination of  $\alpha,\beta$ -unsaturated carboxylic acids. *Tetrahedron Lett.* **2018**, *59*, 4593–4596. [[CrossRef](#)]
29. Jayaraman, A.; Cho, E.; Kim, J.; Lee, S. Decarboxylative Tribromination for the Selective Synthesis of Tribromomethyl Ketone and Tribromovinyl Derivatives. *Adv. Synth. Catal.* **2018**, *360*, 3978–3989. [[CrossRef](#)]
30. Zhang, X.; Feng, X.; Zhang, H.; Yamamoto, Y.; Bao, M. Transition-metal-free decarboxylative halogenation of 2-picolinic acids with dihalomethane under oxygen conditions. *Green Chem.* **2019**, *21*, 5565–5570. [[CrossRef](#)]
31. Yang, Y.; Zhang, L.; Deng, G.J.; Gong, H. Simple, Efficient and Controllable Synthesis of Iodo/Di-Iodoarenes via Ipso iododecarboxylation/Consecutive Iodination Strategy. *Sci. Rep.* **2017**, *7*, 40430.
32. Fu, Z.; Li, Z.; Song, Y.; Yang, R.; Liu, Y.; Cai, H. Decarboxylative Halogenation and Cyanation of Electron-Deficient Aryl Carboxylic Acids via Cu Mediator as Well as Electron-Rich Ones through Pd Catalyst under Aerobic Conditions. *J. Org. Chem.* **2016**, *81*, 2794–2803. [[CrossRef](#)]
33. Jiang, M.; Yang, H.; Jin, Y.; Ou, L.; Fu, H. Visible-Light-Induced Decarboxylative Iodination of Aromatic Carboxylic Acids. *Synlett* **2018**, *29*, 1572–1577.
34. Patra, T.; Mukherjee, S.; Ma, J.; Strieth-Kalthoff, F.; Glorius, F. Visible-Light-Photosensitized Aryl and Alkyl Decarboxylative Functionalization Reactions. *Angew. Chem. Int. Ed.* **2019**, *58*, 10514–10520; *Angew. Chem.* **2019**, *131*, 10624–10630. [[CrossRef](#)] [[PubMed](#)]
35. Fu, Z.; Jiang, Y.; Jiang, L.; Li, Z.; Guo, S.; Cai, H. Cu-catalyzed decarboxylative iodination of aryl carboxylic acids with NaI: A practical entry to aryl iodides under aerobic conditions. *Tetrahedron Lett.* **2018**, *59*, 4458–4461. [[CrossRef](#)]
36. Li, Z.; Wang, K.; Liu, Z.-Q. Transition-Metal-Free Hunsdiecker Reaction of Electron-Rich Arene-carboxylic Acids and Aryl Aldehydes in Water. *Synlett* **2014**, *25*, 2508–2512. [[CrossRef](#)]
37. Perry, G.J.P.; Quibell, J.M.; Panigrahi, A.; Larrosa, I. Transition-Metal-Free Decarboxylative Iodination: New Routes for Decarboxylative Oxidative Cross-Couplings. *J. Am. Chem. Soc.* **2017**, *139*, 11527–11536. [[CrossRef](#)]
38. Quibell, J.M.; Perry, G.J.P.; Cannas, D.M.; Larrosa, I. Transition-metal-free decarboxylative bromination of aromatic carboxylic acids. *Chem. Sci.* **2018**, *9*, 3860–3865. [[CrossRef](#)]
39. Chen, C.; Tong, X. Synthesis of organic halides via palladium(0) catalysis. *Org. Chem. Front.* **2014**, *1*, 439–446. [[CrossRef](#)]
40. Petrone, D.A.; Ye, J.; Lautens, M. Modern Transition-Metal-Catalyzed Carbon–Halogen Bond Formation. *Chem. Rev.* **2016**, *116*, 8003–8104. [[CrossRef](#)]
41. Jones, D.J.; Lautens, M.; McGlacken, G.P. The emergence of Pd-mediated reversible oxidative addition in cross coupling, carbonylation and carbonylation reactions. *Nat. Catal.* **2019**, *2*, 843–851. [[CrossRef](#)]
42. Echavarren, A.M.; Stille, J.K. Palladium-Catalyzed Coupling of Aryl Triflates with Organostannanes. *J. Am. Chem. Soc.* **1987**, *109*, 5478–5486. [[CrossRef](#)]



43. Roy, A.H.; Hartwig, J.F. Reductive Elimination of Aryl Halides from Palladium(II). *J. Am. Chem. Soc.* **2001**, *123*, 1232–1233. [[CrossRef](#)]
44. Roy, A.H.; Hartwig, J.F. Directly Observed Reductive Elimination of Aryl Halides from Monomeric Arylpalladium(II) Halide Complexes. *J. Am. Chem. Soc.* **2003**, *125*, 13944–13945. [[CrossRef](#)] [[PubMed](#)]
45. Roy, A.H.; Hartwig, J.F. Reductive Elimination of Aryl Halides upon Addition of Hindered Alkylphosphines to Dimeric Arylpalladium(II) Halide Complexes. *Organometallics* **2004**, *23*, 1533–1541. [[CrossRef](#)]
46. Shen, X.; Hyde, A.M.; Buchwald, S.L. Palladium-Catalyzed Conversion of Aryl and Vinyl Triflates to Bromides and Chlorides. *J. Am. Chem. Soc.* **2010**, *132*, 14076–14078. [[CrossRef](#)]
47. Pan, J.; Wang, X.; Zhang, Y.; Buchwald, S.L. An Improved Palladium-Catalyzed Conversion of Aryl and Vinyl Triflates to Bromides and Chlorides. *Org. Lett.* **2011**, *13*, 4974–4976. [[CrossRef](#)]
48. Sather, A.C.; Buchwald, S.L. The Evolution of Pd<sup>0</sup>/Pd<sup>II</sup>-Catalyzed Aromatic Fluorination. *Acc. Chem. Res.* **2016**, *49*, 2146–2157. [[CrossRef](#)]
49. Newman, S.G.; Lautens, M. The Role of Reversible Oxidative Addition in Selective Palladium(0)-Catalyzed Intramolecular Cross-Couplings of Polyhalogenated Substrates: Synthesis of Brominated Indoles. *J. Am. Chem. Soc.* **2010**, *132*, 11416–11417. [[CrossRef](#)]
50. Newman, S.G.; Lautens, M. Palladium-Catalyzed Carboiodination of Alkenes: Carbon–Carbon Bond Formation with Retention of Reactive Functionality. *J. Am. Chem. Soc.* **2011**, *133*, 1778–1780. [[CrossRef](#)]
51. Liu, H.; Li, C.; Qiu, D.; Tong, X. Palladium-Catalyzed Cycloisomerizations of (Z)-1-Iodo-1,6-dienes: Iodine Atom Transfer and Mechanistic Insight to Alkyl Iodide Reductive Elimination. *J. Am. Chem. Soc.* **2011**, *133*, 6187–6193. [[CrossRef](#)]
52. Chen, C.; Hou, L.; Cheng, M.; Su, J.; Tong, X. Palladium(0)-Catalyzed Iminohalogenation of Alkenes: Synthesis of 2-Halomethyl Dihydropyrroles and Mechanistic Insights into the Alkyl Halide Bond Formation. *Angew. Chem. Int. Ed.* **2015**, *54*, 3092–3096, *Angew. Chem.* **2015**, *127*, 3135–3139. [[CrossRef](#)]
53. Chen, X.; Zhao, J.; Dong, M.; Yang, N.; Wang, J.; Zhang, Y.; Liu, K.; Tong, X. Pd(0)-Catalyzed Asymmetric Carbohalogenation: H-Bonding-Driven C(sp<sup>3</sup>)-Halogen Reductive Elimination under Mild Conditions. *J. Am. Chem. Soc.* **2021**, *143*, 1924–1931. [[CrossRef](#)]
54. Lee, Y.H.; Morandi, B. Palladium-Catalyzed Intermolecular Aryliodination of Internal Alkynes. *Angew. Chem. Int. Ed.* **2019**, *58*, 6444–6448; *Angew. Chem.* **2019**, *131*, 6510–6515. [[CrossRef](#)] [[PubMed](#)]
55. Boehm, P.; Kehl, N.; Morandi, B. Rhodium-Catalyzed Anti-Markovnikov Transfer Hydroiodination of Terminal Alkynes. *Angew. Chem. Int. Ed.* **2023**, *62*, e202214071; *Angew. Chem.* **2023**, *135*, e202214071. [[CrossRef](#)] [[PubMed](#)]
56. Hao, W.; Wei, J.; Geng, W.; Zhang, W.-X.; Xi, Z. Transfer of Aryl Halide to Alkyl Halide: Reductive Elimination of Alkylhalide from Alkylpalladium Halides Containing *syn*-β-Hydrogen Atoms. *Angew. Chem. Int. Ed.* **2014**, *53*, 14533–14537; *Angew. Chem.* **2014**, *126*, 14761–14765. [[CrossRef](#)] [[PubMed](#)]
57. Guo, L.; Rueping, M. Transition-Metal-Catalyzed Decarbonylative Coupling Reactions: Concepts, Classifications, and Applications. *Chem. Eur. J.* **2018**, *24*, 7794–7809. [[CrossRef](#)]
58. Zhao, Q.; Szostak, M. Redox-Neutral Decarbonylative Cross-Couplings Coming of Age. *ChemSusChem* **2019**, *12*, 2983–2987. [[CrossRef](#)]
59. Lu, H.; Yu, T.-Y.; Xu, P.-F.; Wei, H. Selective Decarbonylation via Transition-Metal-Catalyzed Carbon–Carbon Bond Cleavage. *Chem. Rev.* **2021**, *121*, 365–411. [[CrossRef](#)]
60. Lalloo, N.; Bringham, C.E.; Sanford, M.S. Mechanism-Driven Development of Group 10 Metal-Catalyzed Decarbonylative Coupling Reactions. *Acc. Chem. Res.* **2022**, *55*, 3430–3444. [[CrossRef](#)]
61. Keaveney, S.T.; Schoenebeck, F. Palladium-Catalyzed Decarbonylative Trifluoromethylation of Acid Fluorides. *Angew. Chem. Int. Ed.* **2018**, *57*, 4073–4077, *Angew. Chem.* **2018**, *130*, 4137–4141. [[CrossRef](#)]
62. Okuda, Y.; Xu, J.; Ishida, T.; Wang, C.-A.; Nishihara, Y. Nickel-Catalyzed Decarbonylative Alkylation of Aryl Fluorides Assisted by Lewis-Acidic Organoboranes. *ACS Omega* **2018**, *3*, 13129–13140. [[CrossRef](#)]
63. Wang, Z.; Wang, X.; Nishihara, Y. Nickel-catalysed decarbonylative borylation of aryl fluorides. *Chem. Commun.* **2018**, *54*, 13969–13972. [[CrossRef](#)]
64. Wang, X.; Wang, Z.; Liu, L.; Asanuma, Y.; Nishihara, Y. Nickel-Catalyzed Decarbonylative Stannylation of Acyl Fluorides under Ligand-Free Conditions. *Molecules* **2019**, *24*, 1671. [[CrossRef](#)] [[PubMed](#)]
65. Wang, X.; Wang, Z.; Nishihara, Y. Nickel/copper-cocatalyzed decarbonylative silylation of acyl fluorides. *Chem. Commun.* **2019**, *55*, 10507–10510. [[CrossRef](#)] [[PubMed](#)]
66. Fu, L.; Chen, Q.; Wang, Z.; Nishihara, Y. Palladium-Catalyzed Decarbonylative Alkylation of Acyl Fluorides. *Org. Lett.* **2020**, *22*, 2350–2353. [[CrossRef](#)]
67. Chen, Q.; Fu, L.; Nishihara, Y. Palladium/copper-cocatalyzed decarbonylative alkynylation of acyl fluorides with alkynylsilanes: Synthesis of unsymmetrical diarylethynes. *Chem. Commun.* **2020**, *56*, 7977–7980. [[CrossRef](#)] [[PubMed](#)]

68. Chen, Q.; Fu, L.; You, J.; Nishihara, Y. Nickel-Catalyzed Decarbonylative Alkynylation of Acyl Fluorides with Terminal Alkynes under Copper-Free Conditions. *Synlett* **2021**, 32, 1560–1564.
69. You, J.; Chen, Q.; Nishihara, Y. Nickel-Catalyzed Decarbonylative Thioetherification of Acyl Fluorides via C–F Bond Activation. *Synthesis* **2021**, 53, 3045–3050.
70. Chen, Q.; Li, Z.; Nishihara, Y. Palladium/Copper-Cocatalyzed Arylsilylation of Internal Alkynes with Acyl Fluorides and Silylboranes: Synthesis of Tetrasubstituted Alkenylsilanes by Three-Component Coupling Reaction. *Org. Lett.* **2022**, 24, 385–389. [[CrossRef](#)]
71. Chen, Q.; You, J.; Tian, T.; Li, Z.; Kashiwara, M.; Mori, H.; Nishihara, Y. Nickel-Catalyzed Decarbonylative Reductive Alkylation of Aryl Fluorides with Alkyl Bromides. *Org. Lett.* **2022**, 24, 9259–9263. [[CrossRef](#)]
72. Tian, T.; Chen, Q.; Li, Z.; Nishihara, Y. Recent Advances in C–F Bond Activation of Acyl Fluorides Directed toward Catalytic Transformation by Transition Metals, *N*-Heterocyclic Carbenes, or Phosphines. *Synthesis* **2022**, 54, 3667–3697.
73. Malapit, C.A.; Bour, J.R.; Brigham, C.E.; Sanford, M.S. Base-free nickel-catalysed decarbonylative Suzuki–Miyaura coupling of acid fluorides. *Nature* **2018**, 563, 100–104. [[CrossRef](#)]
74. Malapit, C.A.; Bour, J.R.; Laursen, S.R.; Sanford, M.S. Mechanism and Scope of Nickel-Catalyzed Decarbonylative Borylation of Carboxylic Acid Fluorides. *J. Am. Chem. Soc.* **2019**, 141, 17322–17330. [[CrossRef](#)] [[PubMed](#)]
75. Laloo, N.; Malapit, C.A.; Taimoory, S.M.; Brigham, C.E.; Sanford, M.S. Decarbonylative Fluoroalkylation at Palladium(II): From Fundamental Organometallic Studies to Catalysis. *J. Am. Chem. Soc.* **2021**, 143, 18617–18625. [[CrossRef](#)] [[PubMed](#)]
76. Fehér, P.P.; Stirling, A. Theoretical Study on the Formation of Ni(PR<sub>3</sub>)(Aryl)F Complexes Observed in Ni-Catalyzed Decarbonylative C–C Coupling of Acyl Fluorides. *Organometallics* **2020**, 39, 2774–2783. [[CrossRef](#)]
77. Ogiwara, Y.; Sakurai, Y.; Hattori, H.; Sakai, N. Palladium-Catalyzed Reductive Conversion of Acyl Fluorides via Ligand-Controlled Decarbonylation. *Org. Lett.* **2018**, 20, 4204–4208. [[CrossRef](#)]
78. Sakurai, S.; Yoshida, T.; Tobisu, M. Iridium-catalyzed Decarbonylative Coupling of Acyl Fluorides with Arenes and Heteroarenes via C–H Activation. *Chem. Lett.* **2019**, 48, 94–97. [[CrossRef](#)]
79. Kayumov, M.; Zhao, J.-N.; Mirzaakhmedov, S.; Wang, D.-Y.; Zhang, A. Synthesis of Arylstannanes via Palladium-Catalyzed Decarbonylative Coupling of Aryl Fluorides. *Adv. Synth. Catal.* **2020**, 362, 776–781. [[CrossRef](#)]
80. Sakurai, S.; Tobisu, M. Palladium-catalyzed Decarbonylative Cyanation of Acyl Fluorides and Chlorides. *Chem. Lett.* **2021**, 50, 151–153. [[CrossRef](#)]
81. He, B.; Liu, X.; Li, H.; Zhang, X.; Ren, Y.; Su, W. Rh-Catalyzed General Method for Directed C–H Functionalization via Decarbonylation of in-Situ-Generated Acid Fluorides from Carboxylic Acids. *Org. Lett.* **2021**, 23, 4191–4196. [[CrossRef](#)]
82. Blanchard, N.; Bizet, V. Acid Fluorides in Transition-Metal Catalysis: A Good Balance between Stability and Reactivity. *Angew. Chem. Int. Ed.* **2019**, 58, 6814–6817; *Angew. Chem.* **2019**, 131, 6886–6889. [[CrossRef](#)]
83. Ogiwara, Y.; Sakai, N. Acyl Fluorides in Late-Transition-Metal Catalysis. *Angew. Chem. Int. Ed.* **2020**, 59, 574–594; *Angew. Chem.* **2020**, 132, 584–605. [[CrossRef](#)]
84. Blum, J.; Lipshes, Z. Catalytic Conversion of Benzoic Anhydrides into Fluorenones. *J. Org. Chem.* **1969**, 34, 3076–3080. [[CrossRef](#)]
85. Zhang, X.; Jordan, F.; Szostak, M. Transition-metal-catalyzed decarbonylation of carboxylic acids to olefins: Exploiting acyl C–O activation for the production of high value products. *Org. Chem. Front.* **2018**, 5, 2515–2521. [[CrossRef](#)]
86. Gooßen, L.J.; Rodríguez, N. A mild and efficient protocol for the conversion of carboxylic acids to olefins by a catalytic decarbonylative elimination reaction. *Chem. Commun.* **2004**, 724–725. [[CrossRef](#)] [[PubMed](#)]
87. Kajita, Y.; Kurahashi, T.; Matsubara, S. Nickel-Catalyzed Decarbonylative Addition of Anhydrides to Alkynes. *J. Am. Chem. Soc.* **2008**, 130, 17226–17227. [[CrossRef](#)]
88. Matsuda, T.; Suzuki, K. Rhodium(III)-catalysed decarbonylative coupling of maleic anhydrides with alkynes. *RSC Adv.* **2014**, 4, 37138–37141. [[CrossRef](#)]
89. Prakash, R.; Shekharrao, K.; Gogoi, S.; Boruah, R.C. Ruthenium-catalyzed decarbonylative addition reaction of anhydrides with alkynes: A facile synthesis of isocoumarins and  $\alpha$ -pyrones. *Chem. Commun.* **2015**, 51, 9972–9974. [[CrossRef](#)]
90. Jin, W.; Yu, Z.; He, W.; Ye, W.; Xiao, W.-J. Efficient Rh(I)-Catalyzed Direct Arylation and Alkenylation of Arene C–H Bonds via Decarbonylation of Benzoic and Cinnamic Anhydrides. *Org. Lett.* **2009**, 11, 1317–1320. [[CrossRef](#)]
91. Maetani, S.; Fukuyama, T.; Ryu, I. Rhodium-Catalyzed Decarbonylative C–H Arylation of 2-Aryloxybenzoic Acids Leading to Dibenzofuran Derivatives. *Org. Lett.* **2013**, 15, 2754–2757. [[CrossRef](#)]
92. Qiu, X.; Wang, P.; Wang, D.; Wang, M.; Yuan, Y.; Shi, Z. P<sup>III</sup>-Chelation-Assisted Indole C7-Arylation, Olefination, Methylation, and Acylation with Carboxylic Acids/Anhydrides by Rhodium Catalysis. *Angew. Chem. Int. Ed.* **2019**, 58, 1504–1508; *Angew. Chem.* **2019**, 131, 1518–1522. [[CrossRef](#)]
93. Han, X.; Yuan, Y.; Shi, Z. Rhodium-Catalyzed Selective C–H Trideuteromethylation of Indole at C7 Position Using Acetic-*d*<sub>6</sub> Anhydride. *J. Org. Chem.* **2019**, 84, 12764–12772. [[CrossRef](#)]

94. Liu, C.; Ji, C.-L.; Zhou, T.; Hong, X.; Szostak, M. Bimetallic Cooperative Catalysis for Decarbonylative Heteroarylation of Carboxylic Acids via C-O/C-H Coupling. *Angew. Chem. Int. Ed.* **2021**, *60*, 10690–10699; *Angew. Chem.* **2021**, *133*, 10785–10794. [[CrossRef](#)] [[PubMed](#)]
95. Stephan, M.S.; Teunissen, A.J.J.M.; Verzijl, G.K.M.; de Vries, J.G. Heck Reactions without Salt Formation: Aromatic Carboxylic Anhydrides as Arylating Agents. *Angew. Chem. Int. Ed.* **1998**, *37*, 662–664; *Angew. Chem.* **1998**, *110*, 688–690. [[CrossRef](#)]
96. Gooßen, L.J.; Paetzold, J.; Winkel, L. Pd-Catalyzed Decarbonylative Heck Olefination of Aromatic Carboxylic Acids Activated in situ with Di-*tert*-butyl Dicarboxylate. *Synlett* **2002**, *10*, 1721–1723. [[CrossRef](#)]
97. O'Brien, E.M.; Bercot, E.A.; Rovis, T. Decarbonylative Cross-Coupling of Cyclic Anhydrides: Introducing Stereochemistry at an  $sp^3$  Carbon in the Cross-Coupling Event. *J. Am. Chem. Soc.* **2003**, *125*, 10498–10499. [[CrossRef](#)] [[PubMed](#)]
98. Gooßen, L.J.; Paetzold, J. New Synthesis of Biaryls via Rh-Catalyzed Decarbonylative Suzuki-Coupling of Carboxylic Anhydrides with Arylboroxines. *Adv. Synth. Catal.* **2004**, *346*, 1665–1668. [[CrossRef](#)]
99. Liu, C.; Ji, C.-L.; Qin, Z.-X.; Hong, X.; Szostak, M. Synthesis of Biaryls via Decarbonylative Palladium-Catalyzed Suzuki-Miyaura Cross-Coupling of Carboxylic Acids. *iScience* **2019**, *19*, 749–759. [[CrossRef](#)]
100. Li, X.; Liu, L.; Huang, T.; Tang, Z.; Li, C.; Li, W.; Zhang, T.; Li, Z.; Chen, T. Palladium-Catalyzed Decarbonylative Sonogashira Coupling of Terminal Alkynes with Carboxylic Acids. *Org. Lett.* **2021**, *23*, 3304–3309. [[CrossRef](#)]
101. Liu, C.; Szostak, M. Decarbonylative Sonogashira Cross-Coupling of Carboxylic Acids. *Org. Lett.* **2021**, *23*, 4726–4730. [[CrossRef](#)]
102. Bie, F.; Liu, X.; Szostak, M.; Liu, C. Decarbonylative Alkynylation of Aryl Anhydrides via Palladium Catalysis. *J. Org. Chem.* **2023**, *88*, 4442–4451. [[CrossRef](#)]
103. Liu, C.; Ji, C.-L.; Hong, X.; Szostak, M. Palladium-Catalyzed Decarbonylative Borylation of Carboxylic Acids: Tuning Reaction Selectivity by Computation. *Angew. Chem. Int. Ed.* **2018**, *57*, 16721–16726. [[CrossRef](#)]
104. Zhang, W.; Bie, F.; Ma, J.; Zhou, F.; Szostak, M.; Liu, C. Palladium-Catalyzed Decarbonylative Borylation of Aryl Anhydrides. *J. Org. Chem.* **2021**, *86*, 17445–17452. [[CrossRef](#)] [[PubMed](#)]
105. Li, K.; Li, R.; Cui, Y.; Liu, C. Decarbonylative borylation of aryl anhydrides via rhodium catalysis. *Org. Biomol. Chem.* **2024**, *22*, 1693–1698. [[CrossRef](#)]
106. Zhou, J.-Y.; Tao, S.-W.; Liu, R.-Q.; Zhu, Y.-M. Forging C–S Bonds through Nickel-Catalyzed Aryl Anhydrides with Thiophenols: Decarbonylation or Decarbonylation Accompanied by Decarboxylation. *J. Org. Chem.* **2019**, *84*, 11891–11901. [[CrossRef](#)] [[PubMed](#)]
107. Ji, H.; Cao, H.; Wang, G.; Xing, F.; Szostak, M.; Liu, C. Predominant intermolecular decarbonylative thioetherification of carboxylic acids using nickel precatalysts. *Org. Chem. Front.* **2023**, *10*, 4275–4281. [[CrossRef](#)]
108. Liu, C.; Qin, Z.-X.; Ji, C.-L.; Hong, X.; Szostak, M. Highly-chemoselective step-down reduction of carboxylic acids to aromatic hydrocarbons via palladium catalysis. *Chem. Sci.* **2019**, *10*, 5736–5742. [[CrossRef](#)]
109. Komiya, S.; Yamamoto, A.; Yamamoto, T. Preparation of Acyl(Carboxylato)Nickel and -Palladium Complexes  $M(COR)(OCOR')L_2$  ( $M = Ni, Pd$ ) And Reversible Reductive Elimination of Carboxylic Anhydrides,  $RCOOCOR'$ . *Chem. Lett.* **1981**, *10*, 193–196. [[CrossRef](#)]
110. Sano, K.; Yamamoto, T.; Yamamoto, A. Preparation of new Pt- and Ni-containing Cyclic Esters and Their Reactivities. *Chem. Lett.* **1983**, *12*, 115–118. [[CrossRef](#)]
111. Sano, K.; Yamamoto, T.; Yamamoto, A. Preparation of Ni- or Pt-Containing Cyclic Esters by Oxidative Addition of Cyclic Carboxylic Anhydrides and Their Properties. *Bull. Chem. Soc. Jpn.* **1984**, *57*, 2741–2747. [[CrossRef](#)]
112. Nagayama, K.; Kawataka, F.; Sakamoto, M.; Shimizu, I.; Yamamoto, A. Preparation and Reactivities of Acyl(carboxylato)palladium Complexes. *Chem. Lett.* **1995**, *24*, 367–368. [[CrossRef](#)]
113. Miller, J.A.; Nelson, J.A. Oxidative Addition of Carboxylic Acid Anhydrides to Rhodium(I) Phosphine Complexes To Produce Novel Rhodium(III) Acyl Derivatives. *Organometallics* **1991**, *10*, 2958–2961. [[CrossRef](#)]
114. Lee, Y.H.; Morandi, B. Metathesis-active ligands enable a catalytic functional group metathesis between aryl chlorides and aryl iodides. *Nat. Chem.* **2018**, *10*, 1016–1022. [[CrossRef](#)] [[PubMed](#)]
115. Boehm, P.; Martini, T.; Lee, Y.H.; Cachet, B.; Morandi, B. Palladium-Catalyzed Decarbonylative Iodination of Aryl Carboxylic Acids Enabled by Ligand-Assisted Halide Exchange. *Angew. Chem. Int. Ed.* **2021**, *60*, 17211–17217; *Angew. Chem.* **2021**, *133*, 17348–17355. [[CrossRef](#)] [[PubMed](#)]
116. De La Higuera Macias, M.; Arndtsen, B.A. Functional Group Transposition: A Palladium-Catalyzed Metathesis of Ar–X  $\sigma$ -Bonds and Acid Chloride Synthesis. *J. Am. Chem. Soc.* **2018**, *140*, 10140–10144. [[CrossRef](#)]
117. Tian, T.; Kashihara, M.; Yan, W.; Nishihara, Y. Palladium-Catalyzed Decarbonylative Nucleophilic Halogenation of Acyl Fluorides and Chlorides: Synthesis of Aryl Halides via Reductive Elimination of the C–X ( $X = I, Br, \text{ and } Cl$ ) Bond and Mechanistic Implications. *ACS Catal.* **2024**, *14*, 11905–11917. [[CrossRef](#)]
118. Watson, D.A.; Su, M.; Teverovskiy, G.; Zhang, Y.; García-Fortanet, J.; Kinzel, T.; Buchwald, S.L. Formation of ArF from LPdAr(F): Catalytic Conversion of Aryl Triflates to Aryl Fluorides. *Science* **2009**, *325*, 1661–1664. [[CrossRef](#)]

119. Amatore, C.; Jutand, A.; Suarez, A. Intimate Mechanism of Oxidative Addition to Zerovalent Palladium Complexes in the Presence of Halide Ions and Its Relevance to the Mechanism of Palladium-Catalyzed Nucleophilic Substitutions. *J. Am. Chem. Soc.* **1993**, *115*, 9531–9541. [\[CrossRef\]](#)
120. Miloserdov, F.M.; McMullin, C.L.; Belmonte, M.M.; Benet-Buchholz, J.; Bakmutov, V.I.; Macgregor, S.A.; Grushin, V.V. The Challenge of Palladium-Catalyzed Aromatic Azidocarbonylation: From Mechanistic and Catalyst Deactivation Studies to a Highly Efficient Process. *Organometallics* **2014**, *33*, 736–752. [\[CrossRef\]](#)
121. Miloserdov, F.M.; Grushin, V.V. Palladium-Catalyzed Aromatic Azidocarbonylation. *Angew. Chem. Int. Ed.* **2012**, *51*, 3668–3672; *Angew. Chem.* **2012**, *124*, 3728–3732. [\[CrossRef\]](#)
122. Malapit, C.A.; Ichiishi, N.; Sanford, M.S. Pd-Catalyzed Decarbonylative Cross-Couplings of Aryl Chlorides. *Org. Lett.* **2017**, *19*, 4142–4145. [\[CrossRef\]](#)
123. Liao, W.-J.; Lin, S.-Y.; Kuo, Y.-S.; Liang, C.-F. Site-Selective Acylation of Phenols Mediated by a Thioacid Surrogate through Sodium Thiosulfate Catalysis. *Org. Lett.* **2022**, *24*, 4207–4211. [\[CrossRef\]](#)
124. Daskiewicz, J.-B.; Depeint, F.; Viornery, L.; Bayet, C.; Comte-Sarrazin, G.; Comte, G.; Gee, J.M.; Johnson, I.T.; Ndjoko, K.; Hostettmann, K.; et al. Effects of Flavonoids on Cell Proliferation and Caspase Activation in a Human Colonic Cell Line HT29: An SAR Study. *J. Med. Chem.* **2005**, *48*, 2790–2804. [\[CrossRef\]](#) [\[PubMed\]](#)
125. Dhimitruka, I.; SantaLucia, J., Jr. Investigation of the Yamaguchi Esterification Mechanism. Synthesis of a Lux-S Enzyme Inhibitor Using an Improved Esterification Method. *Org. Lett.* **2006**, *8*, 47–50. [\[CrossRef\]](#) [\[PubMed\]](#)
126. Zhang, L.; Xue, X.; Xu, C.; Pan, Y.; Zhang, G.; Xu, L.; Li, H.; Shi, Z. Rhodium-Catalyzed Decarbonylative Direct C2-Arylation of Indoles with Aryl Carboxylic Acids. *ChemCatChem* **2014**, *6*, 3069–3074. [\[CrossRef\]](#)
127. Bashir, I.A.; Lee, S. Base-Mediated Synthesis of Anhydrides from Activated Amides. *J. Org. Chem.* **2023**, *88*, 6159–6167. [\[CrossRef\]](#) [\[PubMed\]](#)
128. Khatun, N.; Santra, S.K.; Banerjee, A.; Patel, B.K. Nano CuO Catalyzed Cross Dehydrogenative Coupling (CDC) of Aldehydes to Anhydrides. *Eur. J. Org. Chem.* **2015**, *2015*, 1309–1313. [\[CrossRef\]](#)
129. Gaspa, S.; Amura, I.; Porcheddu, A.; De Luca, L. Anhydrides from aldehydes or alcohols via oxidative cross-coupling. *New J. Chem.* **2017**, *41*, 931–939. [\[CrossRef\]](#)
130. Agrawal, S.K.; Majhi, P.K.; Goodfellow, A.S.; Tak, R.K.; Cordes, D.B.; McKay, A.P.; Kasten, K.; Bühl, M.; Smith, A.D. Synthesis of Tetra-Substituted 3-Hydroxyphthalide Esters by Isothiourea-Catalysed Acylative Dynamic Kinetic Resolution. *Angew. Chem. Int. Ed.* **2024**, *63*, e202402909; *Angew. Chem.* **2024**, *136*, e202402909. [\[CrossRef\]](#)

**Disclaimer/Publisher’s Note:** The statements, opinions and data contained in all publications are solely those of the individual author(s) and contributor(s) and not of MDPI and/or the editor(s). MDPI and/or the editor(s) disclaim responsibility for any injury to people or property resulting from any ideas, methods, instructions or products referred to in the content.